Human like trajectory generation for a biped robot with a four-bar linkage for the knees

Yannick Aoustin, Arnaud Hamon

Human like trajectory generation for a biped robot with a four-bar linkage for the knees.

Yannick Aoustin and Arnaud Hamon

L'UNAM, Institut de Recherche en Communications et Cybernétique de Nantes, UMR CNRS 6597,
CNRS, École Centrale de Nantes, Université de Nantes, 1 rue de la Noë, BP 92101. 44321 Nantes, Cedex 3, France

Abstract

The design of a knee joint is a key issue in robotics to improve the locomotion and the performances of the bipedal robots. We study a design for the knee joints of a planar bipedal robot, based on a four-bar linkage. We design walking reference trajectories composed of double support phases, single support phases and impacts. The single support phases are divided in two sub-phases. During the first sub-phase the stance foot has a flat contact with the ground. During the second sub-phase the stance foot rotates on its toes. In the double support phase, both stance feet rotate. This phase is ended by an impact on the ground of the toe of the forward foot, the rear foot taking off. The single support phase is ended by an impact of the heel of the swing foot, the other foot keeping contact with the ground through its toes. A parametric optimization problem is presented for the determination of the parameters corresponding to the optimal cyclic walking gaits. In the optimization process this novel bipedal robot is successively, overactuated (double support with rotation of both stance feet), fully actuated (single support sub-phase with a flat foot contact), and underactuated (single support sub-phase with a rotation of the stance foot). A comparison of the performances with respect to a sthenic criterion is proposed between a biped equipped with four-bar knees and the other with revolute joints. Our numerical results show that the performances with a four-bar linkage are badder for the smaller velocities and better for the higher velocities. These

Email address: corresponding author: yannick.aoutsin@irccyn.ec-nantes.fr (Yannick Aoustin and Arnaud Hamon)

numerical results allows us to think that the four-bar linkage could be a good technological way to increase the speed of the future bipedal robots.

Keywords: Bipedal robot, Walking gait, Four-bar linkage, Parametric Optimisation, Underactuation.

1. Introduction

Since several years Researchers in robotics have done many efforts to develop walking robots, especially bipedal robots. Experimental bipedal robots are composed of links, which can be connected through actuated revolute joints, see for example Rabbit [1] and Mabel [2], or through actuated prismatic joints, such as the biped with telescopic legs developed by Grishin *et al.* [3]. T. Yang *et al.* [4] use a compliant parallel knee to improve the walking motion. Several authors also deal with the walking and running gaits using the toe rotation [5], [6], and [7]. However from biomechanics studies a lot the understanding of the human lower limb is improved, and especially the knee joint [8] and the ankle joint [9]. Indeed, these two joints have a complex architecture formed by non symmetric surfaces. Their motion is more complex than a revolute joint motion. The motions of the femur with respect to the tibia are limited due to the patella and many ligaments. In addition to the flexion in the sagittal plane, there is an internal rotation with a displacement of the Instantaneous Center of Rotation (ICR) of the knee joint and a posterior translation of the femur on the tibia. These motions are guided by the cruciate ligaments and the articular contact [10], [8]. These motions cannot be represented by one or two revolute joints. Different studies have confirmed these results by an observation of the motions of the human knee in the 3D space [11]. Consequently, for bipedal robots complex knee joints appear with a displacement of their Instantaneous Center of Rotation (ICR), see G. Gini et al. [12]. They use knee joints based on the human knee surfaces. F. Wang et al. [13] have developed a bipedal robot with two different joints, a revolute joint and a four-bar linkage. However, the singularities of the common four-bar linkage, i.e., non crossed four-bar linkage, usually limit the flexion of the knee. On the contrary, the flexion of the knee joint based on a crossed four-bar linkage is usually less limited with the kinematic singularities. One possible advantage of a four-bar linkage for the knee joints would be to reduce the consumption of energy. In [14] it is shown from optimal walking gaits that a knee based on a four-bar linkage is better than a knee designed with a

revolute joint in terms of energy consumption. However these walking gaits are very simple and not realistic because each step is composed of a single support phase ended with an instantaneous double support phase to define the impact the swing foot on the ground.

This paper aims to study the performance of a planar bipedal robot equipped with knees based on crossed four-bar linkages for a more realistic walking gait composed of double support phases, single support sub-phases with a flat foot contact, and single support sub-phases with a rotation of the foot around its toe. The works of [15], [16], [17], and [18], show that the presence of toe joints allows to perform longer strides, climb higher steps, reduce the energy consumption and walk at a higher speed. This biped robot is fully actuated in single support sub-phase with a flat foot contact. It is underactuated in single support sub-phase with a rotation of the stance foot around its toes. And it is overactuated in double support phase with a feet rotation on the front heel and the rear toe. We developed a parametric optimization method, which takes into account these previous characteristics, to define a set of optimal cyclic reference trajectories. We studied a sthenic criterion, which relates to the driving torques of the biped robot, for different speeds. The main contribution of this paper is to obtain a set of dynamical stable walking gaits with double support phases, impacts, and single support phases for this bipedal biped. A comparison with a bipedal robot, which is equipped with revolute knee joints show that the four-bar linkage could preserve the torques of the actuators for the higher speeds. The paper is organized as follows. Section 2 presents the novel planar bipedal robot whose knees are based on four-bar linkages. Section 3 is devoted to the biped modeling with specific difficulties due to the four-bar linkage of each knee. Section 4 deals with the trajectory planning. Section 5 presents numerical results on the walking reference trajectories. Finally, Section 6 offers our conclusion and several perspectives.

2. Presentation of the Bipedal Robot with Knees Composed of a Four-bar Linkage

Let us introduce the bipedal robot, which is depicted in Figure 1. Table 1 gathers the physical data of the biped, which are taken from *Hydroid*, an experimental humanoid robot [18].

The dimensions of the four-bar linkage are chosen with respect to the human characteristics measured by J. Bradley *et al.* through radiography in

	Mass (kg)	Length (m)	Inertia $(kg.m^2)$	Center of mass (m)
foot	$m_f = 0.678$	$L_p = 0.207$ $l_p = 0.072$ $H_p = 0.064$	0.002	$s_{px} = 0.0135$ $s_{py} = 0.0321$
shin	2.188	0.392	0.028	$s_1 = s_4 = 0.169$
thigh	5.025	0.392	0.066	$s_2 = s_3 = 0.169$
trunk	29.27	0.403	0.815	$s_5 = 0.192$
four-bar knee	$m_d = 1.2$	$l_a = AB = 0.029\ m$ $l_b = BC = 0.035\ m$ $l_c = CD = 0.015\ m$ $l_d = AD = 0.025\ m$		

Table 1: Physical parameters of the bipedal robot.

[19].

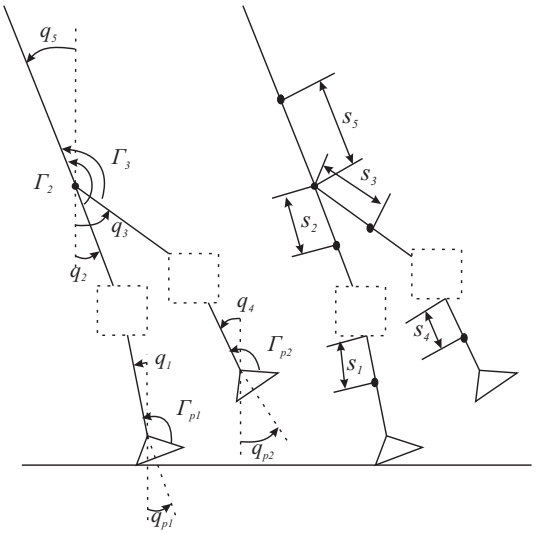

Figure 1: Schematic of the planar bipedal robot. Absolute angular variables and torques.

Figures 1, 2(a), and 2(b) depict the bipedal robot under study and its four-bar knee linkage. Figure 2(a) represents the four-bar knee linkage. The

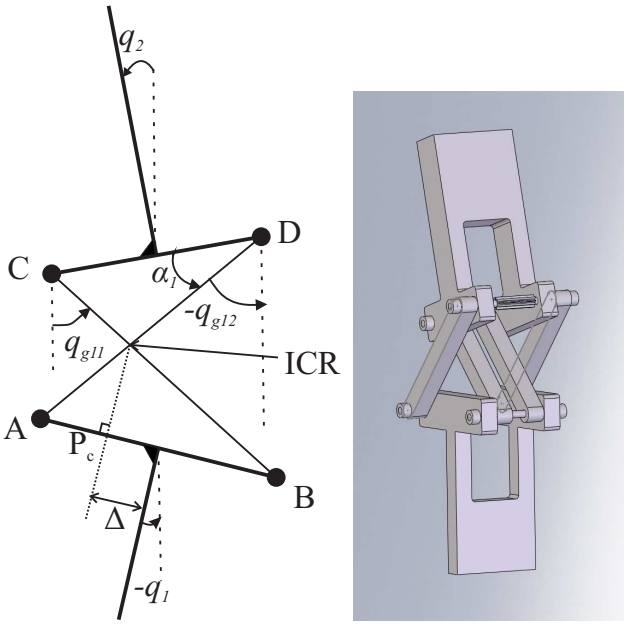

(a) (b)

Figure 2: Details of the four-bar joint and position of the Instantaneous Center of Rotation (ICR)

angular variable α_1 is the actuated variable of the four-bar linkage.

3. The Biped Modeling

3.1. General dynamic model in double support phase

The bipedal robot is equipped with two closed-loop knees. Let us introduce the constraint equations solving the dynamic model [20]. Equations for the knee joints 1 and 2 are similar. For a sake of clarity we consider the knee joint 1 only. The equations of the closed-loop geometric constraints are defined as follows:

$$\begin{aligned} l_a \cos\, q_1 - l_b \sin\, q_{g_{11}} + l_c \cos\, q_2 + l_d \sin\, q_{g_{12}} = 0 \\ l_a \sin\, q_1 + l_b \cos\, q_{g_{11}} + l_c \sin\, q_2 - l_d \cos\, q_{g_{12}} = 0. \end{aligned} \tag{1}$$

Their first and second time derivatives are:

$$\begin{aligned} -l_a \dot{q}_1 \sin\, q_1 - l_b \dot{q}_{g_{11}} \cos\, q_{g_{11}} - l_c \dot{q}_2 \sin\, q_2 + l_d \dot{q}_{g_{12}} \cos\, q_{g_{12}} = 0 \\ l_a \dot{q}_1 \cos\, q_1 - l_b \dot{q}_{g_{11}} \sin\, q_{g_{11}} + l_c \dot{q}_2 \cos\, q_2 + l_d \dot{q}_{g_{12}} \sin\, q_{g_{12}} = 0, \end{aligned} \tag{2}$$

and

$$\begin{array}{c} -l_a\ddot{q}_1 \sin\, q_1 - l_b\ddot{q}_{g_{11}} \cos\, q_{g_{11}} - l_c\ddot{q}_2 \sin\, q_2 + l_d\ddot{q}_{g_{12}} \cos\, q_{g_{12}} - \\ l_a\dot{q}_1^2 \cos\, q_1 + l_b\dot{q}_{g_{11}}^2 \sin\, q_{g_{11}} - l_c\dot{q}_2^2 \cos\, q_2 - l_d\dot{q}_{g_{12}}^2 \sin\, q_{g_{12}} = 0 \\ \\ l_a\ddot{q}_1 \cos\, q_1 - l_b\ddot{q}_{g_{11}} \sin\, q_{g_{11}} + l_c\ddot{q}_2 \cos\, q_2 + l_d\ddot{q}_{g_{12}} \sin\, q_{g_{12}} - \\ l_a\dot{q}_1^2 \sin\, q_1 - l_b\dot{q}_{g_{11}}^2 \cos\, q_{g_{11}} - l_c\dot{q}_2^2 \sin\, q_2 + l_d\dot{q}_{g_{12}}^2 \cos\, q_{g_{12}} = 0. \end{array} \tag{3}$$

Through the virtual work principle, these constraints equations can be expressed in the dynamic model by adding the Lagrange multipliers $\mathbf{J}_{e_1}^{\mathrm{t}}\lambda$. Here $\mathbf{J_{e_1}}$ is the 2×13 Jacobian matrix such as equations (2) and (3) can be rewritten under the compact forms:

$$\mathbf{J}_{e_1}\dot{\mathbf{x}} = \mathbf{0} \tag{4}$$

and

$$\mathbf{J}_{e_1}\ddot{\mathbf{x}} + \dot{\mathbf{J}}_{e_1}\dot{\mathbf{x}} = \mathbf{0}. \tag{5}$$

and vector $\boldsymbol{\lambda} = \mathbf{f_{c_1}} = [f_{x_1}, f_{y_1}]^{\mathrm{t}}$ defines the constraint force for the loop closure of the four-bar mechanism of the knee 1 (see Figure 2(a)). The generalized vector $\mathbf{x}$ is such as

$$\mathbf{x} = [q_{p_1}, q_{p_2}, q_1, \cdots, q_5, q_{g_{11}}, q_{g_{12}}, q_{g_{21}}, q_{g_{22}}, x_h, y_h]^{\mathrm{t}}.$$

Here x_h and y_h are the hip coordinates. We apply the same principle for the knee joint 2 to obtain the biped modeling with the four-bar linkage for the knees:

$$\mathbf{A}_e(\mathbf{x})\ddot{\mathbf{x}} + \mathbf{h}_e(\mathbf{x}, \dot{\mathbf{x}}) = \begin{bmatrix}\mathbf{D}_e & \mathbf{J}_{e_1}^{\mathrm{t}} & \mathbf{J}_{e_1}^{\mathrm{t}}\end{bmatrix}\begin{bmatrix}\boldsymbol{\Gamma} \\ \mathbf{f_c}\end{bmatrix} + \mathbf{J}_{r_1}^{\mathrm{t}}\begin{bmatrix}\mathbf{r}_1 \\ \mathbf{m}_{1_z}\end{bmatrix} + \mathbf{J}_{r_2}^{\mathrm{t}}\begin{bmatrix}\mathbf{r}_2 \\ \mathbf{m}_{2_z}\end{bmatrix}, \tag{6}$$

with the constraint equations,

$$\begin{array}{c} \mathbf{J}_{r_i}\ddot{\mathbf{x}} + \dot{\mathbf{J}}_{r_i}\dot{\mathbf{x}} = \mathbf{0} \text{ for } i = 1 \text{ to } 2, \\ \\ \begin{bmatrix}\mathbf{J}_{e_1} \\ \mathbf{J}_{e_2}\end{bmatrix}\ddot{\mathbf{x}} + \begin{bmatrix}\dot{\mathbf{J}}_{e_1} \\ \dot{\mathbf{J}}_{e_2}\end{bmatrix}\dot{\mathbf{x}} = \mathbf{0}. \end{array} \tag{7}$$

$\boldsymbol{\Gamma} = [\Gamma_{p_1}, \Gamma_{p_2}, \Gamma_1, \Gamma_2, \Gamma_3, \Gamma_4]^{\mathrm{t}}$ is the vector of the applied joint torques, $\begin{bmatrix}\mathbf{r}_i & \mathbf{m}_{i_z}\end{bmatrix}^{\mathrm{t}}$, with $i = 1$ to 2, are the resultant wrenchs of the contact efforts with the ground reaction in both feet, and $\mathbf{f_c} = [\mathbf{f}_{\mathbf{c_1}}^{\mathrm{t}}, \mathbf{f}_{\mathbf{c_2}}^{\mathrm{t}}]^{\mathrm{t}}$. $\mathbf{J}_{r_1}$ and $\mathbf{J}_{r_2}$ are the 3×13 Jacobian matrices for the constraint equations in position and orientation

for both feet, respectively. $\mathbf{A}_e(\mathbf{x})$ is the 13×13 symmetric positive definite inertia matrix, $\mathbf{h}_e(\mathbf{x}, \dot{\mathbf{x}})$ is the 13×1 vector, which groups the centrifugal, Coriolis effects, and the gravity forces. $\mathbf{D}_e$ is a 13×6 matrix, consisting of zeros and units, which is given through the principle of virtual work [21].

This dynamic model (6) with constraints (7) is valid in single support and double support phases. During a single support phase the ground reaction force is zero on the swing foot.

3.2. Reduced model in single support phase

The aim is to propose a dynamic model with an implicit liaison of the stance foot with the ground to calculate the torques during the optimization process, with the knowledge of the reference trajectories for the generalized coordinates. This reduced dynamic model is only valid if the stance foot does not take off, and there is no sliding during the swing phase.

Then, during the single support phase, the stance foot is assumed to remain on the ground, *i.e.*, there is no sliding motion and no take-off. We can use a new generalized vector $\mathbf{q} = [q_{p_1}, q_{p_2}, q_1, \cdots, q_5, q_{g_{11}}, q_{g_{12}}, q_{g_{21}}, q_{g_{22}}]^{\mathrm{t}}$. The reduced dynamic model does not depend on the ground reaction force, which is applied in the stance foot. The dynamic model in single support phase for the biped equipped with the four-bar knees is given by:

$$\mathbf{A}(\mathbf{q})\ddot{\mathbf{q}} + \mathbf{h}(\mathbf{q}, \dot{\mathbf{q}}) = \begin{bmatrix} \mathbf{D} & \mathbf{J}_1^{\mathrm{t}} & \mathbf{J}_2^{\mathrm{t}} \end{bmatrix} \begin{bmatrix} \mathbf{\Gamma} \\ \mathbf{f}_c \end{bmatrix}, \tag{8}$$

with the constraints equation,

$$\begin{bmatrix} \mathbf{J}_1 \\ \mathbf{J}_2 \end{bmatrix} \ddot{\mathbf{q}} + \begin{bmatrix} \dot{\mathbf{J}}_1 \\ \dot{\mathbf{J}}_2 \end{bmatrix} \dot{\mathbf{q}} = \mathbf{0}. \tag{9}$$

Here the sizes of matrices are such that $\mathbf{A} = \mathbf{A}(9 \times 9)$, $\mathbf{h} = \mathbf{h}(9 \times 1)$, $\mathbf{D} = \mathbf{D}(9 \times 6)$, $\mathbf{J}_1 = \mathbf{J}_1(2 \times 9)$, and $\mathbf{J}_2 = \mathbf{J}_2(2 \times 9)$.

To define the constraints about the ground reaction with the flat foot contact, see Figure 3, we recall the calculation of position of the Zero Momentum Point. The resultant force $\mathbf{f}_r$ of the ground reaction can be calculated by applying the second Newton law at the center of mass of the biped:

$$m\boldsymbol{\gamma} = \mathbf{f}_r + m\mathbf{g}. \tag{10}$$

Here m is the global mass of the biped, $\boldsymbol{\gamma} = [\ddot{x}_g, \ddot{y}_g]^{\mathrm{t}}$ are the horizontal and vertical components of the acceleration for its center of mass in the world

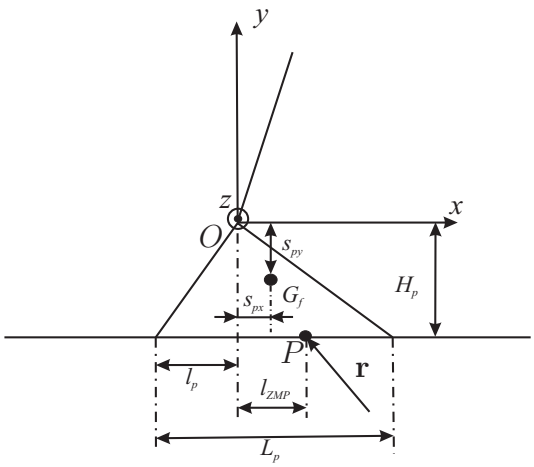

Figure 3: Details of the foot.

frame. $\mathbf{g} = [0, -g]^{\mathrm{t}}$ is the vector of the acceleration of the gravity. This equation allows directly to get $\mathbf{r}$ during the single support phase. Assuming the center of mass G_f of the foot has for coordinates (s_{px}, s_{py}), see Figure 3. Let m_f be the mass of the foot. The resultant of the reaction efforts of the ground acting in any point P of the foot is defined $\mathbf{r} = [f_{r_x}, f_{r_y}, m_z]^{\mathrm{t}}$. Point P is called the Zero Moment Point if $m_z = 0$. One necessary and sufficient condition to have a flat foot contact is, that P belongs to the convex hull of the supporting area (Vukobratovic [22]). In this case the ZMP is merged with the center of pressure. For the planar biped the coordinate of the ZMP can be obtained through the calculation of the global equilibrium of the bipedal robot around axis z, which gives:

$$l_{ZMP} = \frac{\Gamma_{p_1} + s_{px} m_f g - H_p f_{r_x}}{f_{r_y}}, \tag{11}$$

where Γ_{p_1} is the applied torque on the ankle. When the stance foot rotates around its toes the ZMP is merged with this toe.

To calculate the applied joint torques and the sthenic criterion for the bipedal robot during the optimization process, we use the dynamic model (8).

We assume the friction effects due to the four-bar mechanism are negligible with respect to those in the gearbox of the actuators. Then only the performances of actuators are considered to calculate the sthenic criterion for

the biped equipped with the four-bar linkage for the knee joints. No friction terms are included in the model.

3.3. Impact model

During the biped's gait, impacts occur, when the sole, the heel, or the toe of the swing foot touches the ground. Let T be the instant of an impact. We assume that the impact is absolutely inelastic and that the foot does not slip. Given these conditions, the ground reactions at the instant of an impact can be considered as impulsive forces and defined by Dirac delta-functions $\mathbf{r}_j = \mathbf{i}_j \delta(t - T)$ $(j = 1, 2)$. Here $\mathbf{i}_j = [i_{jx},\, i_{jy},\, i_{jz}]^{\mathrm{t}}$ is the magnitudes vector of the impulsive reaction in the foot j (see [23]). Impact equations can be obtained through the integration of the matrix motion equation (6) for the infinitesimal time from T^- to T^+. The torques provided by the actuators in the joints, Coriolis, and gravity forces have finite values. Thus they do not influence the impact. Consequently, the impact equations can be written in the following matrix form:

$$\mathbf{A}_e(\mathbf{x}(T))(\dot{\mathbf{x}}^+ - \dot{\mathbf{x}}^-) = \begin{bmatrix} \mathbf{J}_{e_1}^{\mathrm{t}} & \mathbf{J}_{e_2}^{\mathrm{t}} \end{bmatrix} \mathbf{i}_{f_c} + \mathbf{J}_{r_1}^{\mathrm{t}} \mathbf{i}_1 + \mathbf{J}_{r_2}^{\mathrm{t}} \mathbf{i}_2. \tag{12}$$

Here $\mathbf{x}(T)$ denotes the configuration of the biped at the instant $t = T$, (this configuration does not change at the instant of the impact), $\dot{\mathbf{x}}^-$ and $\dot{\mathbf{x}}^+$ are respectively the velocity vectors just before and just after an inelastic impact. To take into account the closed-loop of the four-bar knee linkage we have to complete (12) with:

$$\begin{bmatrix} \mathbf{J}_{e_1} \\ \mathbf{J}_{e_2} \end{bmatrix} \dot{\mathbf{x}}^+ = \mathbf{0}. \tag{13}$$

The velocity of the contact part of the stance foot $(j = 1)$ before an impact is null,

$$\mathbf{J}_{r_1} \dot{\mathbf{x}}^- = \mathbf{0}. \tag{14}$$

The swing foot $(j = 2)$ after the impact becomes a stance foot. Therefore, the velocity of its contact part with the ground becomes zero after the impact,

$$\mathbf{J}_{r_2} \dot{\mathbf{x}}^+ = \mathbf{0}. \tag{15}$$

Generally speaking, two results are possible after the impact, if we assume that there is no slipping of the stance feet. The stance foot lifts off the ground or both feet remain on the ground. In the first case, the vertical component

of the velocity of the taking-off foot just after the impact must be directed upwards. Also there is no interaction (no friction, no sticking) between the taking-off foot and the ground. The ground reaction in this taking-off leg tip must be null. In the second case, the stance foot velocity has to be zero just after the impact. The ground produces impulsive reactions (generally, $\mathbf{i}_j \neq 0$, $j = 1, 2$) and the vertical components of the impulsive ground reactions in both feet are directed upwards. For the second case, the passive impact equation (12) must be completed with the following matrix equations:

$$\mathbf{J}_{r_1}\dot{\mathbf{x}}^+ = \mathbf{0}. \tag{16}$$

Generally, the result of an impact depends on two factors: the biped's configuration at the instant of an impact and the direction of the swing foot velocity just before impact [23]. After an impact for a biped, there are two possible phases: a single support or a finite time double support.

The resolution of the system composed of (12), (13), (15), and eventually (16) gives the velocity vector $\dot{\mathbf{x}}^+$ just after the impact, the impulsive ground reaction efforts $\mathbf{i}_1$, $\mathbf{i}_2$, and the impulsive forces $\mathbf{i}_{f_c} = [\mathbf{i}^{\mathrm{t}}_{f_{c1}}, \mathbf{i}^{\mathrm{t}}_{f_{c2}}]^{\mathrm{t}}$ relatively to the velocity vector $\dot{\mathbf{x}}^-$ just before the impact.

To calculate the position of the ZMP at the impact with flat foot, we have to take into account the impulsive ground reaction in the global equilibrium of the stance foot and the result is:

$$l_{ZMP} = -\frac{H_p\ i_{jx}}{i_{jy}}. \tag{17}$$

4. Gait optimization for the cyclic walking

4.1. Principle

The biped is driven by six torques, and its configuration is given by vector $\mathbf{q}$ of generalized coordinates. To transform the optimization problem into a finite dimension problem, the evolution of each degree of freedom of the biped is described through a parametric function. Then for the double support phase and the single support phase with a flat foot contact, the chosen parametric function is a third order polynomial as a function of time. For the single support phase with the rotation of the stance foot, it is a fourth order polynomial as a function of a configuration parameter s.

To insure continuity between two successive phases, the position and velocity of the biped at the beginning and at the end of each phase must be

taken into account with the definition of the parameters of the cubic spline functions.

To design a cyclic walking gait, the behavior of the actuated joint variables are prescribed using third order polynomial functions. The set of parameters are used to calculate these functions, taking into account the properties of continuity between each step. Values for these parameters are calculated by minimizing a sthenic criterion, which relates to the driving torques of the biped robot. Physical conditions of contact between the feet and the ground, and limits on the actuators define non-linear constraints for this optimization process.

4.2. Studied gait

The cyclic walking gait is composed of double support, single support phases, and impacts. In double support phase both feet rotate, see Figures 4a. and 4b, the double support is ended when one foot impacts the ground with its toe, the other foot takes off the ground. The first sub-phase of the single support takes place with a flat foot contact on the ground, see Figure 4c. The second sub-phase of the single support starts with a rotation of the stance foot around its toe. At the end of this single support sub-phase, see Figure 4d, the impacting foot touches the ground with its heel. The other foot keeps contact with the ground through its toe.

During the single support sub-phase with rotation of the stance foot, the biped is underactuated. The time evolution of the biped cannot be directly prescribed without taking into account the dynamic effect of the biped. However to determine the evolution of the biped during this phase, it is possible to parametrize the evolution of each degree of freedom of the biped according to a variable that depends on the biped dynamic [18]. During this single support sub-phase the degrees of freedom of the biped can be presented by the seven first components of vector $\mathbf{q}$, which are q_{p_1}, q_{p_2}, q_1, q_2, q_3, q_4, and q_5. The evolution of each degree of freedom for the biped is chosen as a fourth order polynomial function $p_i(s)$, where s is a configuration parameter

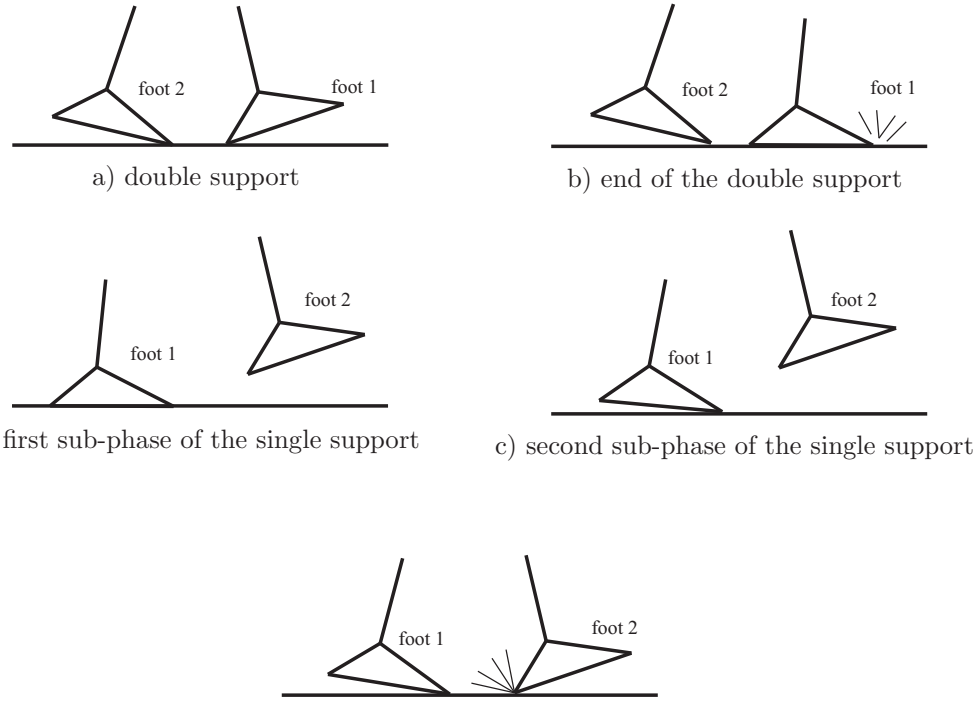

a) double support

b) end of the double support

c) first sub-phase of the single support

c) second sub-phase of the single support

d) end of the single support

Figure 4: Studied walking gait.

varying from 0 to 1, see [24]:

$$\begin{cases} p_i(s) = a_{0_i} + a_{1_i} s + a_{2_i} s^2 + a_{3_i} s^3 + a_{4_i} s^4 \\ \dfrac{\mathrm{d}p_i(s)}{\mathrm{d}s} = a_{1_i} + 2\ a_{2_i} s + 3\ a_{3_i} s^2 + 4\ a_{4_i} s^3 \\ \dfrac{\mathrm{d}^2 p_i(s)}{\mathrm{d}s^2} = 2\ a_{2_i} + 6\ a_{3_i} s + 12\ a_{4_i} s^2. \end{cases} \tag{18}$$

With i is an integer number such as $i = 1, 2, \cdots, 7$. The evolutions of s, $\dot{s}$, and $\ddot{s}$ are obtained by the computation of the angular momentum σ of the biped in the point of contact between the ground and the toe of the stance foot. The angular momentum σ is a linear function with respect to the components of the angular velocities $\dot{\mathbf{q}}(i)$, and its coefficients $I_i(\mathbf{q})$ $(i = 1, ..., 11)$ depend on the vector of the generalized coordinates and the

physical biped parameters.

$$\sigma = \sum_{i=1}^{11} I_i(\mathbf{q})\dot{\mathbf{q}}(i) \tag{19}$$

Through equations (2) and similar equations for the other knee, we can write the following matrix equation:

$$\mathbf{J}_g \ . \ [\dot{q}_{g11}, \dot{q}_{g12}, \dot{q}_{g21}, \dot{q}_{g22}]^{\mathrm{t}} = \mathbf{J} \ . \ [\dot{q}_{p_1}, \dot{q}_{p_2}, \dot{q}_1, \dot{q}_2, \dot{q}_3, \dot{q}_4, \dot{q}_5]^{\mathrm{t}}, \tag{20}$$

where $\mathbf{J}_g = \mathbf{J}_g(4 \times 4)$ and $\mathbf{J} = \mathbf{J}(4 \times 7)$. Then tacking into account (18) and (20) we can write the angular momentum such as,

$$\sigma = (\mathbf{M}_1 + \mathbf{M}_2\mathbf{J}_g^{-1}\mathbf{J})\frac{\mathrm{d}\mathbf{p}(s)}{\mathrm{d}s}\dot{s} \tag{21}$$

Here $\mathbf{M}_1(1 \times 7) = [I_1 \ I_2 \ I_3 \ I_4 \ I_5 \ I_6 \ I_7]$, $\mathbf{M}_2(1 \times 4) = [I_8 \ I_9 \ I_{10} \ I_{11}]$, and $\mathbf{p}(s)(7 \times 1)$ is a vector, that its components are $p_i(s)$, $i = 1, 2, \cdots, 7$. Then for the knee joint 1 tacking into account (18), and from (1) solving the inverse geometrical model through Paul's methods [25] (respectively an identical manner is used for knee joint 2) we can write the angular momentum such as,

$$\sigma(s, \dot{s}) \ = \ I(s)\dot{s} \tag{22}$$

Therefore the angular momentum depends on s and $\dot{s}$ only. Moreover, the dynamic momentum is given by :

$$\dot{\sigma}(s) = -m \ g \ x_g(s) \tag{23}$$

So, we have :

$$\sigma(s, \dot{s}) \ \mathrm{d}\sigma(s) = -m \ g \ x_g(s) \ I(s) \ \mathrm{d}s \tag{24}$$

where g is the gravity acceleration and x_g is the horizontal coordinate of the biped center of mass.
By integration of (24) from 0 to s we obtain:

$$\frac{1}{2}\left[\sigma^2(s, \dot{s}) - \sigma^2(0, \dot{s}_0)\right] = -\int_0^s m \ g \ x_g(\xi) \ I(\xi) \ \mathrm{d}\xi, \tag{25}$$

which gives :

$$\frac{1}{2}I^2(0) \ \dot{s}_0^2 = \frac{1}{2}I^2(s) \ \dot{s}^2 + V(s), \tag{26}$$

where

$$V(s) = m\ g \int_0^s I(\xi) x_g(\xi)\ \mathrm{d}\xi, \tag{27}$$

and $\dot{s}_0$ is the initial velocity for $s = 0$. So, we can determine the evolution of $\dot{s}$ as a function of its initial value $\dot{s}_0$ with :

$$\dot{s} = \frac{\sqrt{I^2(0)\ \dot{s}_0^2 - 2\ V(s)}}{I(s)}. \tag{28}$$

From equations (22) and (23), we obtain $\ddot{s}$:

$$\ddot{s} = \frac{-m\ g\ x_g(s) - \dfrac{\mathrm{d}I(s)}{\mathrm{d}s}\ \dot{s}^2}{I(s)}. \tag{29}$$

4.3. Parametric optimization problem

By parameterizing the joint motion in terms of polynomial functions, the optimization problem is reduced to a constrained optimization problem of the form:

$$\begin{array}{lll} \text{Minimize } C_W & (\mathbf{P}) & \\ \text{subject to } \mathbf{g}_j & (\mathbf{P}) & < 0 \text{ for } j = 1, 2, ...l \end{array} \tag{30}$$

where $\mathbf{P}$ is the set of optimization variables. $C_W(\mathbf{P})$ is the criterion to minimize with l inequality constraints $\mathbf{g}_j(\mathbf{P}) < 0$ to satisfy. The criterion and constraints are given in the following sections.

We used the SQP method (Sequential Quadratic Programming) with the *fmincon* function of Matlab ® to solve this problem, see [26] and [27].

4.3.1. The criterion

Many criteria can be used to produce an optimal trajectory. A sthenic criterion, which relates to the driving torques of the biped robot, is chosen to obtain optimal trajectories:

$$C_W = \frac{1}{d} \int_0^T \Gamma^{\mathrm{t}} \Gamma \mathrm{d}t, \tag{31}$$

where T is the step duration and Γ the vector of the joint torques. During an optimization process the step length d is an optimization variable, and the walking speed v is fixed, such as the step duration is directly given through the relation $T = d/v$.

However, the duration of the single support sub-phase with rotation of the foot cannot be fixed on the optimization process, but the integration of velocity $\dot{s}$ gives the duration of this sub-phase. To set the walking velocity, we add to the optimization criterion the error between the desired speed and the obtained speed with a penalty factor:

$$C = C_W + 10^4(v_d - v) \tag{32}$$

where v_d is the desired velocity and v is the velocity deduced from the step duration.

The resulting optimal control is continuous, and cancels the risks of a jerky functioning [28]. This smoothness property also guarantees a better numerical efficiency for the algorithm used for the optimization problem-solving.

4.3.2. Optimization parameters

To describe the evolution of the articular variable $\mathbf{q}$, we use polynomial functions. During the double support phase the configuration of the biped is described by seven variables, and we use third order polynomial functions to prescribe their trajectories. During the single support sub-phase with a flat foot contact the configuration of the biped is described by six variables, and we use also third order polynomial functions. Finally, for the single support sub-phase with rotation of the foot around its toe, the configuration of the biped is given by seven variables, and we use fourth order polynomial as a function of the configuration parameter s to describe the biped trajectory.

Consequently, the three different functions used to describe the evolution of an articular variable allow to prescribe the initial and final positions and velocities for each phase of a step and an intermediate position during the single support sub-phase with rotation of the foot. The objective of the optimization algorithm is to determine the different initial and final positions, velocities, and an intermediate position to minimize the optimization criterion, and to respect the constraints. To reduce the complexity of this problem and to develop cyclic trajectories we take into account the continuity between the different phases and between the different steps. From the final state of a step to the initial state of the following step, there is an exchange of the number of the joints, since the legs swap their role, we have:

$$q_{p1i} = q_{p2f}, \quad q_{1i} = q_{4f}, \quad q_{2i} = q_{3f}, \quad \text{and} \quad q_{5i} = q_{5f}. \tag{33}$$

Here subscripts i and f mean respectively initial and final.

For the cyclic walking gait there are 47 optimization variables, which are defined through the following vector:

$$\begin{aligned}
\mathbf{P} \;=\; & [q_1(T_{ds}), q_2(T_{ds}), q_5(T_{ds}), q_{p2}(T_{ds}), d, d_0, d_1, d_2, T_{ds}, \\
& \dot{q}_1(T_{ds}), \dot{q}_2(T_{ds}), \dot{q}_5(T_{ds}), \dot{q}_{p1}(T_{ds}), \dot{q}_{p2}(T_{ds}), \\
& q_1(T_{ss}), q_2(T_{ss}), q_3(T_{ss}), q_4(T_{ss}), q_5(T_{ss}), q_{p2}(T_{ss}), T_{ds}, \\
& \dot{q}_1(T_{ss}), \dot{q}_2(T_{ss}), \dot{q}_3(T_{ss}), \dot{q}_4(T_{ss}), \dot{q}_5(T_{ss}), \dot{q}_{p2}(T_{ss}), \\
& q_1((T+T_{ss})/2), q_2((T+T_{ss})/2), q_3((T+T_{ss})/2), q_4((T+T_{ss})/2), \\
& q_5((T+T_{ss})/2), q_{p1}((T+T_{ss})/2), q_{p2}((T+T_{ss})/2), \\
& q_1(T), q_2(T), q_5(T), q_{p1}(T), q_{p2}(T), \\
& \dot{q}_1(T), \dot{q}_2(T), \dot{q}_3(T), \dot{q}_4(T), \dot{q}_5(T), \dot{q}_{p1}(T), \dot{q}_{p2}(T), \dot{s}_0]
\end{aligned} \tag{34}$$

4.3.3. The constraints

Two types of constraints are used to get a realistic gait.

- The necessary constraints, which ensure a valid walking gait. The first constraint ensures the supporting leg tip does not take off or slide on the ground. So, the ground reaction force is inside a friction cone, defined with the coefficient of friction f:

$$\begin{cases} \max(-f\ r_{iy} - r_{ix}) \leq 0 \\ \max(-f\ r_{iy} + r_{ix}) \leq 0 \end{cases} \tag{35}$$

  $j = 1$ or 2. r_x and r_y are the normal and tangential components of the reaction force. Moreover, we can introduce a constraint on the ground reaction at the impact:

$$\begin{cases} (-f\ i_{1y} - i_{1x}) \leq 0 \\ (-f i_{2y} + i_{2x}) \leq 0 \end{cases} \tag{36}$$

To ensure the non rotation of the supporting foot we introduce a constraint on the ZMP during the single support phase and at the instant of the impact:

$$(l_p - L_p) \leq l_{ZMP} \leq l_p \tag{37}$$

Here L_p is the length of the foot and l_p is the distance between the heel and the ankle along the horizontal axis, see Figure 3.

Just after the impact, the velocity of the taking-off foot should be directed upward. In consequence, the positivity of the vertical component of the velocities for the heel and the toes is added to the set of constraints.

The last constraint allows to ensure the non penetration of the swinging foot in the ground.

- The unnecessary constraints, which ensure a technological realistic gait. We introduced mechanical stops on the joint variables. Moreover, we limited the torques with a constraint, which sets a template of the maximum torque of the motor relatively to the velocity [1].

5. Results

In this part, we use the parametric optimization method, presented previously, to produce a set of optimal reference walking trajectories for the biped with four-bar linkage for the knees.

Figure 5 depicts a stick diagram of one step of a walking gait for a biped's speed, which is equal to 2.2 Km/h. We can see the double support phase, the impact of the toe on the ground of the forward stance foot, the single support sub-phase with a flat foot contact, the rotation of the stance foot in the single support sub-phase and finally the impact of the swing foot on the ground with its heel. The value of the optimization criterion for this gait is $C_\Gamma = 1350\ N^2.m.s$. A small oscillation of the hips can be observed in the sagittal plane of the biped. The trunk is bended forward for the limit configurations and during the walking gait. By analogy to the human walking the rotation of both feet seems natural.

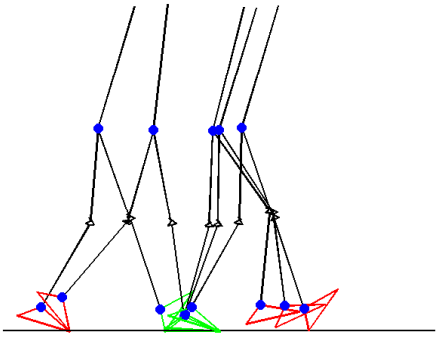

Figure 5: Stick figure plot of one step of walking for a walking velocity of 2.1 Km/h.

Figures 6-10 are devoted to the results about one step of the cyclic walking gaits for a set of several biped's speeds. On figure 6, we can see the comparison of the optimal criterion as a function of the speed for the proposed biped robot and for a biped robot with a revolute knee joint. For the slower speeds until 2.1 Km/h the biped robot with a revolute knee joint seems to be a better solution than the proposed biped robot. After the values of the optimal criteria are smaller for the biped robot equipped with four-bar knees. Consequently, the four-bar knees could be an efficient manner to improve the performances of the future biped robots.

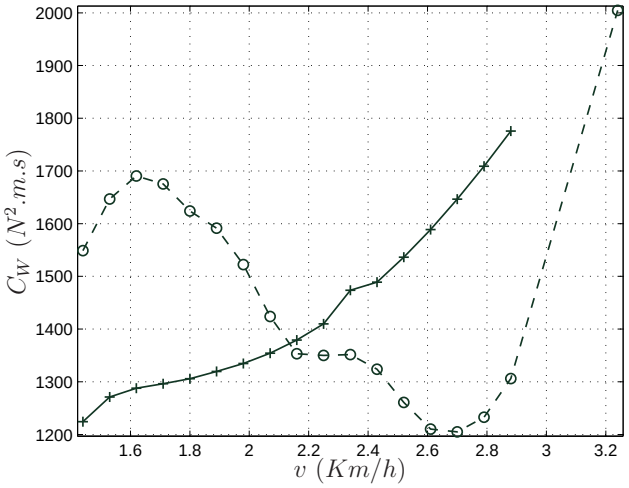

Figure 6: Optimal criteria C_W as a function of the speed for two bipeds: the proposed biped robot (dashed line) and a biped with a revolute knee joint (solid line).

Figure 7 gives the orientation of the support foot at the end of the step as a function of the speeds. The variation in amplitude of this final orientation is relatively small, between -18^o and -24^o for all the speeds.

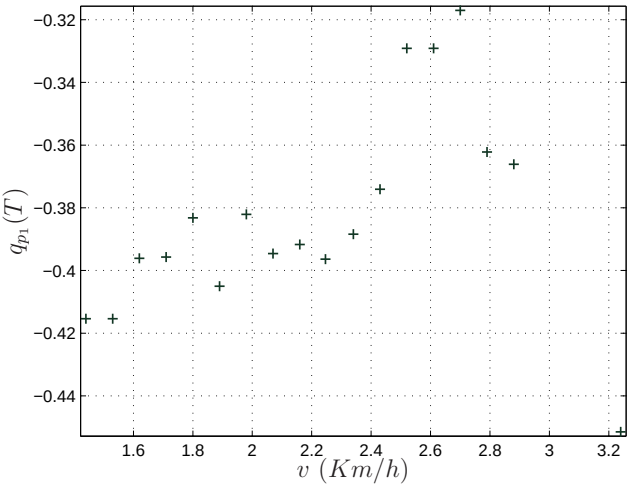

Figure 7: Evolution of the orientation of the support foot at the end of the step as a function of the speed.

Figures 8 and 9 show that the biggest part of the optimal criterion is used for the single support sub-phase with rotation of the stance foot. The rest of the optimal criterion is distributed equally between the double support phase and the sub-phase support with a flat foot on the ground.

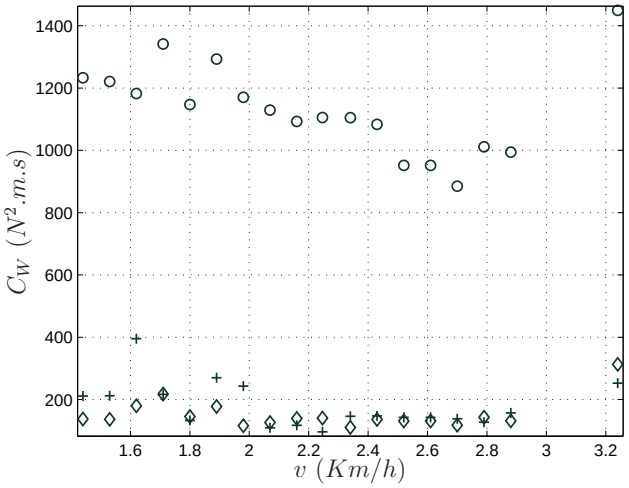

Figure 8: Evolution of the part of the optimal criterion for the double support phase (plus marker), the first single support sub-phase (diamond marker), and the final single support sub-phase (round marker) as a function of the speed.

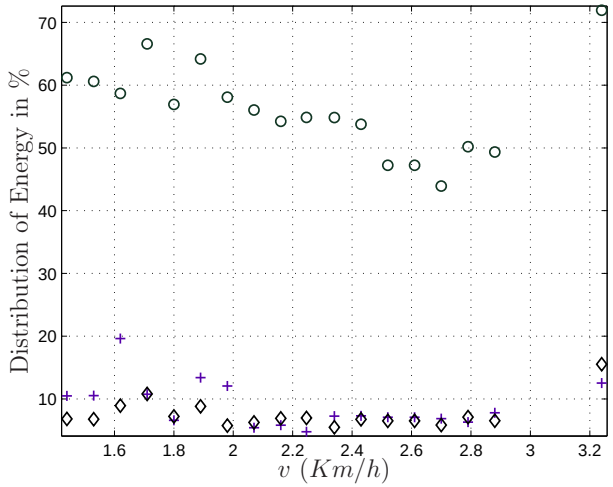

Figure 9: Ratio of the optimal criterion devoted to the double support phase (plus marker), to the first single support sub-phase (diamond marker), and to the second sub-phase of the single support (round marker) as a function of the speed.

Figure 10 shows that when the biped's speed increases, the durations for the double support phase and the sub-phase with a flat foot contact on the ground are quasi constant. The duration of the sub-phase support with a rotation of the stance foot on its toe decreases when the biped's speed increases.

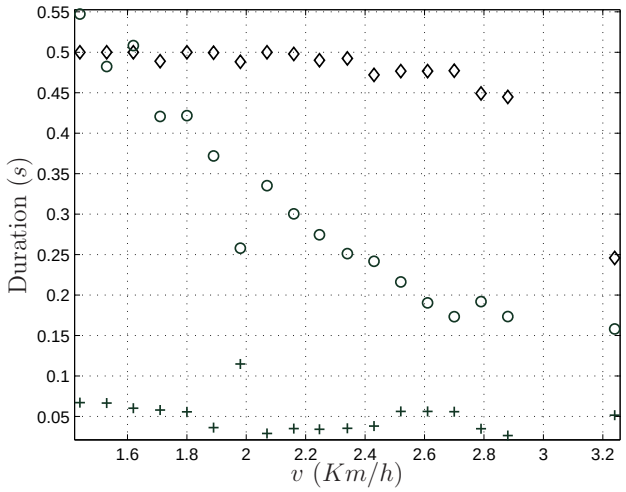

Figure 10: Durations as function of the speeds, of the double support phase (plus marker), of the first sub-phase of the single support (diamond marker), and of the second sub-phase of the single support (round marker).

To summarize the optimization process uses as adjustment variable the duration of the sub-phase support with a rotation of the stance foot around its toe when the biped's speed increases. With the four-bar knees there is a "comfortable" walking gait for a speed, which is close to 2.7 Km/h. For human being, the average speed for a "comfortable" walking is close to 4.0 Km/h. There is a progress margin, may be in the definition of the actuators through the introduction of artificial muscles, elastic elements for example.

6. Conclusion

The main contribution of this paper is to design a novel complex walking for a biped robot with a four-bar linkage for the knees. This novel walking

gait is composed of a double support phase, where the biped is overactuated, a single support sub-phase with a flat foot contact on the ground, the biped being fully actuated, and a single support sub-phase with a rotation of the stance foot. In this last phase the biped is underactuated. A model of the impulsive impacts are presented and used during the transition of the different phases. The numerical tests lead to think that this walking gait for the studied biped robot is feasible in practice. The numerical results show that the performances with a four-bar linkage are badder for the small velocities and better for the higher velocities. Despite these mixed results the four-bar linkage could be a good technological way to increase the speed of the future bipedal robots. Furthermore they have shown that this original biped can performed human like walking with a rotation of the foot without actuation of the toe during the single support phase. In perspective of this work an extension in $3D$ can be done. An optimization problem should be useful to define the optimal length of each bar of the four-bar linkage to increase the work space, without kinematic singularities, of the joint knees. Different orientations of the tibia and the femur with respect to four-bar linkage, should be explored. They are currently fixed to 90^o. Moreover, a comparison of the walking trajectories obtained for an experimental biped with the human movements should proved the higher compatibility with a four-bar linkage than a classical biped equipped with revolute knee joints.

7. ACKNOWLEDGMENTS

This work is supported by ANR grants for the R2A2.

[1] C. Chevallereau, G. Abba, Y. Aoustin, F. Plestan, E. Westervelt, C. Canuddas-de Wit, J. Grizzle, Rabbit: a testbed for advanced control theory, IEEE Control Systems Magazine 23 (5) (2003) 57–79.

[2] K. Sreenath, H. W. Park, I. Poulakakis, J. W. Grizzle, A compliant hybrid zero dynamics controller for stable, efficient and fast bipedal walking on mabel, The International Journal of Robotics Research 30 (9) (2011) 1170–1193.

[3] A. Grishin, A. Formal'sky, A. Lensky, S. Zhitomirsky, Dynamic walking of a vehicle with two telescopic legs controlled by two drives, The International Journal of Robotics Research 13 (2) (1994) 137–147.

[4] T. Yang, E. Westervelt, J. Schmideler, R. Bockbrader, Design and control of a planar bipedal robot ernie with parallel knee compliance, Autonomous robots 25 (2008) 317–333.

[5] S. Kajita, K. Kaneko, M. Morisawa, S. Nakaoka, H. Hirukawa, Zmp-based biped running enhanced by toe springs, in: 2007 IEEE International Conference on Robotics and Automation, 2007, pp. 3963–3969.

[6] R. Tajima, D. Honda, K. Suga, Fast running experiments involving a humanoid robot, in: 2009 IEEE Conference on Robotics and Automation, 2009, pp. 1571–1576.

[7] D. Tlalolini Romero, Y. Aoustin, C. Chevallereau, Design of a walking cyclic gait with single support phases and impacts for the locomotor system of a thirteen-link 3d biped using the parametric optimization, Multibody System Dynamics 23 (1) (2009) 33–56.

[8] D. R. Wilson, J. D. Feikes, J. O'Connor, Ligaments and articular contact guide passive knee flexion, Journal of Biomechanics 31 (1998) 1127–1136.

[9] A. Leardini, J. O'Connor, F. Catani, S. Giannini, A geometric model of the human ankle joint, Journal of Biomechanics 32 (6) (1999) 585 – 591.

[10] F. K. Fuss, Anatomy of the cruciate ligaments and their function in extension and flexion of the human knee joint, American Journal of Anatomy 184 (2) (1989) 165–176.

[11] B. Landjerit, M. Bisserie, Cinématique spatiale de l'articulation fémorotibiale du genou humain : caractérisation expérimentale et implications chirurgicales, Acta Orthopaedica Belgica 58 (2) (1992) 147–158.

[12] G. Gini, U. Scarfogliero, M. Folgheraiter, Human-oriented biped robot design : insights into the development of a truly antropomophic leg, in: IEEE International Conference on Robotics and Automation, 2007, pp. 2910–2915.

[13] F. Wang, C. Wu, Y. Zhang, X. Xu, Design and implementation of coordinated control strategy for biped robot with heterogeneous legs, in: IEEE International Conference on Mechatronics and Automation, 2007, pp. 1559–1564.

[14] A. Hamon, Y. Aoustin, Cross four-bar linkage for the knees of a planar bipedal robot, in: 2010 IEEE-RAS International Conference on Humanoid Robots, 2010, pp. 379–384.

[15] K. Nishiwaka, S. Kagami, Y. Kuniyoshi, M. Inaba, H. Inoue, Toe joints that enhance bipedal and full-body motion of humanoid robots, in: Proceedings of the IEEE International Conference on Robotics and Automation, 2004, pp. 3105–3110.

[16] S. Takao, H. Ohta, Y. Yokokohji, T. Yoshikawa, Functional analysis of human-like mechanical foot, using mechanically constraints shoes, in: Proceedings of the IEEE/RSJ International Conference on Robotics and Automation, 2004, pp. 3847–3852.

[17] J. W. Yoon, N. Handharu, G. Kim, A biorobotic toe, foot and heel models of a biped robot fore more natural walking, in: Proceedings of the IASTED International Conference on Modeling, Identification and Control, 2007.

[18] D. Tlalolini Romero, C. Chevallereau, Y. Aoustin, Comparison of different gaits with rotation of the feet for a planar biped, Robotics and Autonomous Systems 57 (4) (2009) 371–383.

[19] J. Bradley, D. FitzPatrick, D. Daniel, T. Shercliff, J. O'Connor, Orientation of the cruciate ligament in the sagittal plane, The Journal of bone and joint surgery 70-B (1988) 94–99.

[20] W. Khalil, E. Dombre, Modeling, identification and control of robots, Hermes Sciences Europe, 2002.

[21] P. Appell, Dynamique des Systèmes - Mécanique Analytique, Gauthiers-Villars, 1931.

[22] M. Vukobratovic, J. Stepanenko, On the stability of anthropomorphic systems, Mathematical Biosciences 15 (1) (1972) 1–37.

[23] A. Formal'skii, Locomotion of Anthropomorphic Mechanisms, [In Russian], Nauka, Moscow, Russia, 1982.

[24] C. Chevallereau, A. Formal'skii, D. Djoudi, Tracking of a joint path for the walking of an under actuated biped, Robotica 22 (1) (2003) 15–28.

[25] R. Paul, Robot manipulators: mathematics, programming, and control, MIT Press, 1981.

[26] P. Gill, W. Murray, M. Wright, Practical optimization, Academic Press, London, 1981.

[27] M. Powell, Variable metric methods for constrained optimization, Lecture Notes in Mathematics, Springer Berlin / Heidelberg, 1977, pp. 62–72.

[28] C. Chevallereau, G. Bessonnet, G. Abba, Y. Aoustin, Bipedal Robots, ISTE Wiley, 2009.